Colloids and Surfaces A: Physicochem. Eng. Aspects 489 (2016) 378–391

Contents lists available at ScienceDirect

Colloids and Surfaces A: Physicochemical and Engineering Aspects

journal homepage: www.elsevier.com/locate/colsurfa

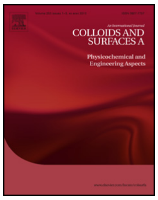

Role of interactions between cationic polymers and surfactants for foam properties

Z. Mitrinova[a], S. Tcholakova[a,*], N. Denkov[a], K.P. Ananthapadmanabhan[b]

[a] *Department of Chemical Engineering, Faculty of Chemistry and Pharmacy, Sofia University, 1 James Bourchier Ave., 1164 Sofia, Bulgaria*
[b] *Unilever Global Research Center, Trumbull, CT 06611, USA*

HIGHLIGHTS

- Effect of cationic polymers on foam properties of SLES + CAPB ± MAc was studied.
- Lupasol polymers bind strongly the MAc molecules in the bulk solution.
- Lupasol polymers reduce MAc activity and its adsorption on the bubble surfaces.
- Merquat 740 affects strongly the foam yield stress, foam-wall friction, behavior of BS + MAc films.
- Merquat 100 with very high charge density has week effect on foam properties.

GRAPHICAL ABSTRACT

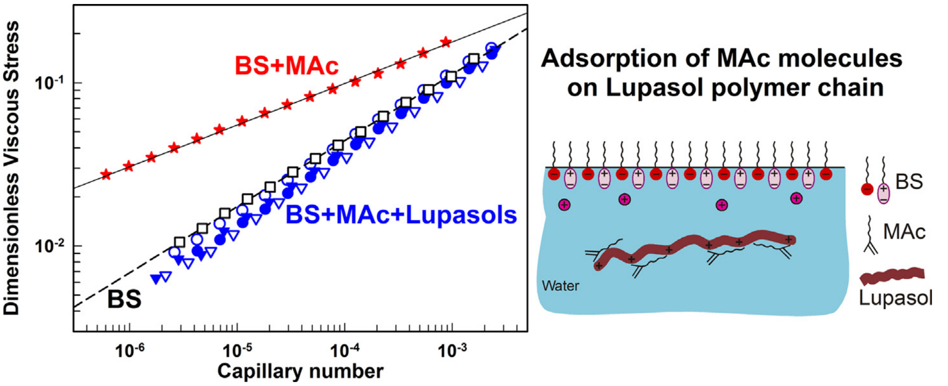

ARTICLE INFO

Article history:
Received 28 August 2015
Received in revised form 19 October 2015
Accepted 20 October 2015
Available online 26 October 2015

Keywords:
Surface dilatational modulus
Cationic polymers
Co-surfactant
Foam rheology
Foam film thinning

ABSTRACT

We study the effect of two classes of cationic polymers, Lupasols (based on polyethylenimine, PEI) and Merquats (based on diallyldimethyl ammonium chloride, DADMAC), on the surface and rheological properties of foams, stabilized with the mixture of anionic (SLES) and zwiterionic (CAPB) surfactants, with and without myristic acid (MAc) present as a cosurfactant. The effects of several polymers from each class, with different molecular mass and charge density, are compared. Polymers from Lupasol series were found to suppress the cosurfactant effect of MAc on all surface and foam properties studied—surface rheological properties, inside foam friction, foam-wall friction, and mean bubble size. The obtained results show that Lupasol polymers bind strongly the MAc molecules in the bulk solution, thus reducing MAc surface activity and adsorption. The cosurfactant effect of MAc could be restored at neutral pH, after increasing MAc concentration to reach a certain weight ratio of MAc/Lupasol. Merquat 740, which is a co-polymer of DADMAC and acrylamide with low charge density, affects strongly the dimensionless foam yield stress, foam-wall friction, and thinning behavior of BS + MAc films. This effect is explained with the strong interactions between polymer molecules and MAc in the mixed adsorption layer at the air–water interface—a relatively thick polymer adsorption layer is formed, able to bridge neighbouring surfaces. In contrast, Merquat 100 with very high charge density (homopolymer of DADMAC) has week effect on foam properties, due to the formation of relatively thin adsorption layers. Thus we observe a variety of possible scenario, depending on (1) the competition between the binding of surfactant/cosurfactant to the polymer molecules in the bulk solution with the polymer adsorption on the bubble surface, and (2) on the ability of the polymer to form thick adsorption layers, bridging the surfaces of neighbouring bubbles.

© 2015 Elsevier B.V. All rights reserved.

---

[*] Corresponding author. Fax: +359 2 962 5643.
E-mail address: sc@lcpe.uni-sofia.bg (S. Tcholakova).

http://dx.doi.org/10.1016/j.colsurfa.2015.10.034
0927-7757/© 2015 Elsevier B.V. All rights reserved.

1. Introduction

Polymer–surfactant mixtures are widely used in many practical applications, such as the paper industry, and home and personal care products [1,2]. Due to their wide-spread usage and complex physico-chemical properties, these systems have attracted the attention of researchers and they are subject of numerous studies, aimed at determining the role of the surfactant–polymer interactions, both in the bulk and on the solution surface, for the overall system behaviour [1–22]. In the course of these studies, it was shown that presence of polymers in surfactant solutions affects significantly the structure and composition of the adsorption layers [6–8,9–12], the thinning behaviour of the respective foam films [14,15,18,19] and the rheological properties of the formed mixed adsorption layers [8,14,16,17], which in turn affects the foamability and foam stability for polymer–surfactant solutions [21,22].

Other important additives in the practical formulations are the co-surfactants, which are used in relatively low concentration to boost the foam properties. Co-surfactants are usually poorly soluble compounds, which are solubilized in the micelles of the main surfactant and affect the surface and foam properties. In our previous studies [23–25] we found that the addition of fatty acids with chain length between 12 and 16 carbon atoms, as co-surfactants to the mixture of SLES and CAPB (main surfactants, described in Section 2), leads to a significant increase of the dilatational surface modulus of the mixed surfactant solutions [23–25]. This high surface modulus (HSM) was shown to affect significantly the dynamic properties of the foams formed from such triple surfactant mixtures, including foam rheological properties [23–25], the rate and mode of foam film thinning [23], and the rate of bubble Ostwald ripening [26].

Therefore, both polymers and co-surfactants can affect significantly the surface and foam properties for mixed polymer/surfactant/co-surfactant solutions. In our recent study [27] we investigated the effect of two cationic polymers, Jaguar C13s and Merquat 100, on the rheological properties of foams, stabilized by the mixture SLES + CAPB, in presence of five different co-surfactants. We showed that the addition of Jaguar to the foaming solutions leads to: (1) significant increase of the foam yield stress for all systems studied; (2) presence of consecutive maximum and minimum in the rheological curve stress vs. shear rate, for foams stabilized by co-surfactants with high surface modulus; (3) presence of significant foam-wall yield stress for all foaming solutions. These effects were explained with the formation of polymer bridges between the neighbouring bubbles in slowly sheared foams (for inside foam friction) and between the bubbles and the confining solid wall (for foam-wall friction). However, the addition of Merquat 100 did not affect noticeably any of the foam rheological properties studied. The foam film observations and surface tension measurements showed that this polymer adsorbs on the bubble surfaces, but forms thin adsorption layers which do not bridge the surfaces of the foam and wetting films.

To clarify the key molecular characteristics of the polymers, which lead to this very different behaviour of Merquat 100 and Jaguar containing foams, for the current study we performed systematic experiments with a series of cationic polymers, which differ in their chemical structure, molecular mass, and charge density—see Table 1 for description of the polymers studied. We used the same main surfactant base, as in our previous studies—a 2:1 mixture of sodium lauryl-oxyethylene sulfate (SLES) and cocoamidopropyl betaine (CAPB), designated as BS (from “Basic surfactants”). This system exhibited excellent foamability and foam stability, and low surface modulus of the bubbles. To obtain systems with high surface modulus, myristic acid (MAc) was added to the BS solution, as in our previous studies [23–27].

Along with the foam rheological measurements (viscous friction inside foam, foam-wall friction), we determined the viscosity and surface tension of the used solutions, and the size of the bubbles after foam shearing under controlled shear rate, which are all quantities needed to interpret the foam rheological data. Experiments with foam films were also performed to determine the effect of the studied polymers on the film thinning behaviour and on the equilibrium film thickness. In addition, the effects of polymers on the surface rheological properties of BS and BS + MAc solutions were studied by oscillating drop method (ODM).

The paper is organized as follows. The methods and materials are described in Section 2. In Section 3.1 we describe the bulk properties of the solutions studied. In Section 3.2 we describe their surface properties. In Section 3.3 we discuss the effect of polymers on the film thinning behavior. In Sections 3.4–3.5 we describe the results for the effects of polymers on the foam properties. The main conclusions are summarized in Section 4.

2. Materials and methods

2.1. Materials

Two series of polymers are studied, according to their chemical content: (1) Merquat series which contains co-polymers of polydiallyldimethylammonium chloride (DADMAC) and acrylic acid or acrylamide, and (2) Lupasol series which is based on polyethylenimine. Merquat polymers are products of Nalco, whereas Lupasol polymers are products of BASF. The polymer properties are described in Table 1, along with their chemical structure (when available). Merquat 100 is a cationic homopolymer of DADMAC, whereas all other polymers are heteropolymers. Polymers from Merquat series have charge density between 2.6 and 6.2 meq/g and molecular mass between 1.2×10^5 and 1.5×10^6 g/mol. Lupasol molecular mass varied between 800 and 2×10^6 g/mol. Polymers from Lupasol series are highly charged with charge density in the range between 8 and 17 meq/g (the charge density is determined by the producer at pH 4.5). The charge density of Lupasol polymers decreases significantly with increasing pH, but no information from the producer is available for the charge density at pH 10 (the natural pH of these polymers).

The basic surfactant system, denoted as “BS”, is a 2:1 mixture (in weight) of the anionic surfactant sodium lauryl-oxyethylene sulfate, SLES (product of STEPAN Co., with commercial name STEOL CS-170) and the zwitterionic surfactant cocoamidopropyl betaine, CAPB (product of Goldschmith, with commercial name Tego Betaine F50). To increase the surface modulus of the BS system, we added myristic acid (MAc).

The procedures for solution preparation were the following: First, we prepared a stock solution of SLES + CAPB (BS). The weight ratio of the active SLES and CAPB in the studied BS-mixtures was fixed at 2:1 and the total surfactant concentration was $C_{TOT} = 10$ wt%. Mixtures of BS + MAc were prepared by dissolving 0.5 wt% MAc in the concentrated BS solution, under mild stirring and heating at 60 °C. For the foaming experiments, these solutions were diluted 20 times with de-ionized water (1 part of the stock solution of BS and 19 parts of de-ionized water). In the prepared BS or BS + MAc stock solutions, we dissolved up to 2 wt% of Lupasol polymers, applying vigorous stirring on magnetic stirrer. The stirring continued until a homogeneous solution was obtained (at least for 1 h). These stocks solutions were kept at room temperature for further studies. The final solutions of BS ± MAc + Lupasol were prepared by direct dilution of 1 g of the concentrated surfactant-polymer solution with 19 g of de-ionized water (1:20 dilution). Therefore, the concentration of the BS mixture in the foaming solu-

Table 1
Properties of used polymers.

Abbreviation used in the text	Name and molecular mass (where available)	Type	Mw, g/mol	+ Charge density, meq/g	Formula	Producer
Merquat 100	Polydiallyldimethylammonium chloride	DADMAC:AA 100:0 mol:mol	1.5×10^5	6.2	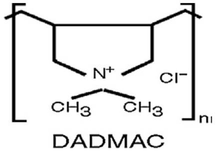	Nalco
Merquat 295	Cationic co-polymer (DADMAC-Acrilic acid)	DADMAC:AA 95:5 mol:mol	1.9×10^5	6.1	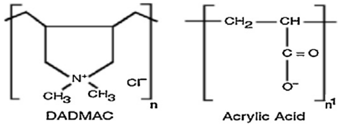	Nalco
Merquat 281	Cationic co-polymer (DADMAC-Acrilic acid)	DADMAC:AA 65:35 mol:mol	4.5×10^5	5.0	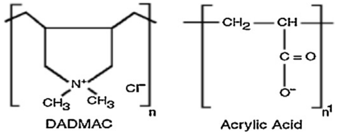	Nalco
Merquat 740	Cationic co-polymer(DADMAC-Acrylamide)	DADMAC:AAm 24:76 mol:mol	1.2×10^5	2.6	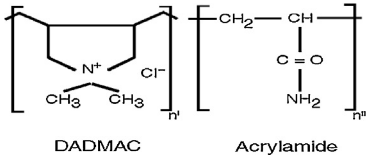	Nalco
Merquat 3330	Polymer of acrylic acid, diallyldimethyl ammonium chloride and acrylamide	Acrylic acid: DADMAC: Acrylamide 35:30:35 mol:mol:mol	15×10^5	3.0	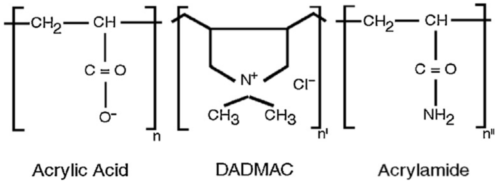	Nalco
Lupasol G10	Polyethylenimine	1/0.9/0.5	800	16		BASF
Lupasol PS	Branched spherical polyamine	1/1.07/0.77	7.5×10^5	17	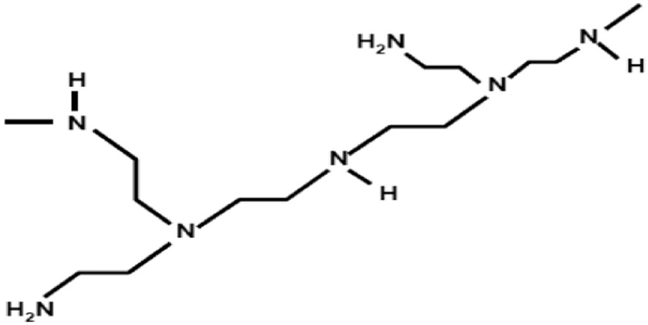	BASF

Table 1 (*Continued*)

Abbreviation used in the text	Name and molecular mass (where available)	Type	+ Charge density, meq/g	Mw, g/mol	Formula	Producer
Lupasol SC-61B	Ethoxylated polyethylenimine	≈80% amine H converted to hydroxyethyl groups	–	1.1×10^5	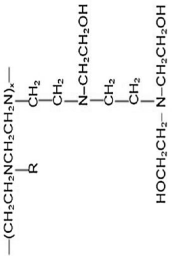	BASF
Lupasol SK	Modified polyethylenimine	–	8	20×10^5		BASF

(1) BASF method, 100% dry at pH 4.

tion was 0.5 wt%, of MAc - 0.025 wt%, and Lupasol polymer was varied between 5×10^{-3} wt% and 0.1 wt%.

Diluted solutions of BS + cosurfactant + Merquat were prepared by mixing 1:1 ratio of polymer solution with BS or BS + MAc solutions with 2-times higher concentrations than needed. The final concentrations in the foaming solutions were 0.5 wt% BS, 0.025 wt% MAc, and the concentration of polymer varied between 5×10^{-3} wt% and 0.1 wt%.

2.2. *Measurements of viscosity and surface tension of the surfactant solutions*

The viscosity of the diluted polymer–surfactant solutions, μ, was measured with thermostated capillary viscometer, after calibration with pure water. The surface tension of the foaming solutions, σ, was measured by Wilhelmy plate method on Tensiometer K100 (Kruss GmbH, Germany) at $T = 20\,^{\circ}$C.

2.3. *Measurements of surface dilatational modulus*

The surface dilatational modulus of the polymer–surfactant solutions was measured by oscillating drop method (ODM) on DSA10 instrument, equipped with ODM/EDM module (Krüss, Germany). The principle of the method is the following: By using a piezo-driven membrane, small oscillations are generated in the volume of a pendant drop (hanged on a needle tip). These oscillations lead to periodical expansions/contractions of the drop surface area: $a(t) = a_0 \sin(\omega t)$, where $a(t) = [A(t) - A_0]/A_0$ is the normalized oscillation of the surface area around its mean value, A_0, while a_0 is the relative amplitude and $\nu = 2\pi\omega$ is the frequency of oscillations. Video-images of the oscillating drop are recorded and analyzed by Laplace equation of capillarity to determine the resulting variation of the surface tension, $\sigma(t)$. For small deformations:

$$\sigma(t) = G_{SD} a_0 \sin(\omega t) + G_{LD} a_0 \cos(\omega t) \qquad (1)$$

where G_{SD} is the surface storage modulus (related to surface dilatational elasticity) and G_{LD} is the surface loss modulus (related to surface dilatational viscosity, $\mu_{SD} = G_{LD}/\omega$). The total surface dilatational modulus is

$$G_D = \left(G_{SD}^2 + G_{LD}^2\right)^{1/2} \qquad (2)$$

In our experiments, the oscillation frequency was fixed at $\nu = 0.2$ Hz, the relative area amplitude was varied between 0.2 and 4%, and the temperature was maintained at $T = 20\,^{\circ}$C using a thermostating chamber (model TC40, Krüss, Germany).

2.4. *Foam generation for rheological measurements*

To generate foam with air volume fraction, $\Phi \approx 0.9$, we used the following procedure: first, 1 mL surfactant solution was sucked into a 20 mL syringe, equipped with a stainless steel needle with 2.5 mm internal diameter (Hamilton, Cat. no. 7730-05). Then 9 mL air was captured in the syringe, forming coarse foam with large bubbles. These large bubbles were broken into much smaller bubbles, by using a series of ejection/injection cycles of the foam through the needle. In this way, foam containing bubbles of sub-millimeter diameter was produced.

2.5. *Determination of bubble size distribution and average bubble size*

Bubble size distribution was determined by using the procedure of Garrett et al. [28,29]. The foam was spread in a small petri dish and an optical triangular prism was placed on top of the plate, in direct contact with the foam. The foam was illuminated by diffuse white light through one of the prism side-walls, whereas the foam observation was made by video-camera, through the other side-wall of the prism. In the recorded images one sees as bright polygonal spots the wetting films, formed between the bubbles and the prism wall, whereas the Plateau borders around the films are seen as dark interconnected areas. The foam images were processed via a shareware computer program Image J, released by the National Institute of Health (NIH).

2.6. Determination of air volume fraction in foam, Φ

The air volume fraction was determined gravimetrically: A syringe with a known volume (20 mL) was filled with foam and weighted. The air volume fraction, Φ, is determined from the relation, $\Phi = 1 - m_F/V_F\rho$,where m_F is the mass of the foam in the syringe, V_F is the volume of this foam, and ρ is the mass density of the foaming solution.

2.7. Characterization of foam rheological properties

Rheological properties of the studied foams were determined with Gemini rotational rheometer (Malvern Instuments, UK), in parallel plate geometry, at temperature of 20 °C.

Two types of experiments were performed—friction inside sheared foam and foam-wall friction. In the first type of experiments, sandpaper (P100) was glued on both plates of the rheometer to suppress foam-wall slip. During the experiment, the shear rate, $\dot{\gamma}$, was varied logarithmically from 0.02 s^{-1} to 200 s^{-1} and the shear stress was recorded, $\tau = \tau(\dot{\gamma})$. In this case, the stress measured by the rheometer was due to viscous dissipation in the bulk of the foam (bubble/bubble friction).

In foam-wall friction experiments, sandpaper (P100) was glued only on the lower plate, whereas a smooth glass plate was glued on the upper (rotating) plate. In this way, there was no slip between the foam and the lower plate, whereas the foam slipped over the upper plate. During these experiments, the shear stress is kept below the foam yield stress to prevent shear flow in the bulk foam. In this way, we can measure the shear stress which is due entirely to the viscous friction of the foam with the confining smooth solid wall (foam-wall friction).

All experiments were performed by using parallel plates with radius of 20 mm, and gap-width of 3 mm. Control experiments at smaller gaps (down to 1.5 mm) did not show any noticeable dependence of the foam rheological properties on the gap-width. No larger gaps were used to avoid possible effects of water drainage from the foam, which could compromise the rheological results.

The obtained results for the dependence of the total shear stress on the rate of strain for steadily sheared foams were described very well by Herschel–Bulkley model, which includes three parameters—yield stress, τ_0; consistency, k; and power-law index, n:

$$\tau = \tau_0 + \tau_V(\dot{\gamma}) = \tau_0 + k\dot{\gamma}^n \tag{3}$$

Here $\dot{\gamma}$ is the applied shear rate, τ is the total shear stress, and τ_V is the viscous stress. As discussed in literature [30–36] it is appropriate to scale the yield stress and viscous stress by the bubble capillary pressure, $P_C \sim \sigma/R_{32}$, whereas the shear rate is adequately represented by the dimensionless capillary number, Ca:

$$\tilde{\tau}_0 = \frac{\tau_0}{(\sigma/R_{32})};\ \tilde{\tau}_V = \frac{\tau_V}{(\sigma/R_{32})};\ Ca = \frac{\mu\dot{\gamma}R_{32}}{\sigma} \tag{4}$$

Here $\tilde{\tau}_0$ is dimensionless yield stress, $\tilde{\tau}_V$ is dimensionless viscous stress, and R_{32} is mean volume-surface radius, while σ is surface tension and μ is viscosity of the foaming solution.

For scaling of the results for foam/wall friction, the dimensionless velocity of the foam with respect to the moving plate and the respective dimensionless foam-wall stress are used [36]:

$$\mathrm{Ca}^* = \frac{\mu V_W}{\sigma} \tag{5}$$

$$\tilde{\tau}_W = \frac{\tau_W}{(\sigma/R_{32})} = C(\mathrm{Ca}^*)^m \tag{6}$$

Here τ_W is viscous wall stress, V_W is velocity of the foam relative to the solid wall, m is power-law index for the foam-wall friction, Ca^* is the dimensionless velocity, which is an equivalent to the capillary number, defined for the experiments of friction inside sheared foam. The power-law index for foam-wall friction takes value $m \approx 1/2$ for tangentially immobile (rigid) bubble surface and $m \approx 2/3$ for bubbles with tangential mobility [36].

These dimensionless quantities are used in the following consideration of the various systems, because they allow one to reveal the non-trivial effects, related to the specific surface properties of the systems.

2.8. Foam films

Foam films of millimetre size were formed and observed in a capillary cell to obtain information for the film-thinning behaviour and equilibrium film thickness. The observations were made by using the method of Scheludko [37]. The films were formed from a biconcave drop, placed in a short capillary (i.d. 2.5 mm, height 3 mm), by sucking out liquid through a side orifice. The observations were performed in reflected monochromatic light, by means of a microscope Axioplan (Zeiss, Germany), equipped with a long-distance objective Zeiss Epiplan 20×/0.40, CCD camera, videorecorder and monitor. Depending on the film thickness, the light reflected by the film has different colours. From the colour and from the intensity of the light reflected from the foam film, one could determine the film thickness with rather good precision [37]. The films that are thicker than 100 nm appear coloured. The films with thickness of about 100 nm appear white (bright), those with thickness of about 50 nm appear gray, and those which thickness is under 30 nm appear dark.

2.9. Size determination of molecular aggregates by dynamic light scattering

Dynamic light scattering (DLS) experiments were conducted on Malvern 4700C goniometric light scattering system (Malvern Instruments, UK) with a solid state laser (532 nm). The hydrodynamic diameter, d_h, of the molecular aggregates (micelles, polymer molecules and/or mixed aggregates) in the studied solutions was determined. DLS experiments were performed at scattering angle of 90°, with additional measurements at 60 and 130° for verification. The multimodal subroutine was used to analyse the experimentally determined autocorrelation function of the scattered light. From the autocorrelation function, the instrument calculates the distribution of the diffusion coefficients of the molecular aggregates in the solution, D. Next, the hydrodynamic diameters of the light scattering aggregates are determined using Stokes–Einstein equation:

$$d_h = \frac{kT}{3\pi\mu D} \tag{7}$$

where k is the Boltzmann constant; T is the absolute temperature, and μ is the dynamic viscosity of the medium. The volume averaged values of the aggregate diameters are used to compare the results for the different systems. Some of the samples were filtered through 100 nm syringe filter but no any effect on the measured aggregate size was detected.

3. Experimental results

In this section we present experimental results about the effects of studied polymers on the bulk solution properties (Section 3.1), surface properties (Section 3.2), film thinning behaviour (Section 3.3), mean bubble size in sheared foams (Section 3.4) and foam rheological properties (Section 3.5).

3.1. Bulk properties

pH of the polymer–surfactant solutions. pH of polymer–surfactant solutions was measured 1 h after their preparation. The obtained results are shown in Table S1 in the supporting information and can be summarized as follows: pH of Merquat-containing solutions is between 5.5 and 6.5 and does not depend significantly on the presence of surfactant in the solution. An exception is the solution of M281 for which pH 3.5 without surfactants, and it increases to 5.5 and 6.5 in the presence of BS or BS + MAc. The lower pH for this polymer is due to the fact that M281 is co-polymer of DADMAC with acrylic acid. The concentration of acrylic acid monomers is ≈2.7 mM which is sufficient to decrease the pH, due to ionization of the acrylic acid monomers. The increase of pH for the polymer–surfactant mixtures is related to the presence of the zwitterionic surfactant CAPB in the surfactant mixture.

pH of Lupasol containing solutions is significantly higher and varies between 9.5 and 10.5 (except for Lupasol SK solutions, where pH is between 7.5 and 8.5). The higher pH of Lupasol-surfactant mixtures is due to water hydrolysis of the Lupasol molecules, which contain primary, secondary and tertiary amines, able to bind H^+, thus releasing free OH^- ions in the solution. In contrast, Merquat polymers have quaternary amine, which is positively charged under all conditions studied and unable to bind additional H^+ ions, so that pH is determined primarily by the surfactant solution.

Therefore, in the data interpretation we should take into account the pH values of the different surfactant-polymer solutions. To compare the effects of Lupasol and Merquat polymers at the same pH, in some series of experiments we decrease the pH of Lupasol-surfactant solutions down to pH 6.5.

Molecular aggregates. We observed the visual appearance of the solutions and measured the size of molecular aggregates by DLS, at 1 h after solution preparation. The obtained results are shown in Table S2.

All polymer solutions (without surfactants) were transparent, although the size of the aggregates varied between 9 nm (M100) and 280 nm (M3330). This observation shows that the polymer aggregates are highly swollen, due to the hydrophilic nature of these polymers. Polymers with low charge density and high molecular mass form bigger aggregates as could be expected.

Mixed polymer–surfactant solutions were clear when the size of aggregates was below 17 nm. Such clear solutions were formed when Merquat polymers with low charge density (below 3.0 meq/g) were used (M740 or M3330) or when Lupasol G10 or Lupasol SC-61B were used. Solutions containing aggregates with size between 25 and 50 nm were slightly opalescent. Such solutions were formed when Merquat polymer with higher charge density of 5.0 meq/g was used (M281), and in presence of Lupasol PS or Lupasol SK. Surfactant-polymer solutions containing Merquat polymer with charge density above 6 meq/g were turbid and the size of the aggregates was above 150 nm. The increase of charge density for Merquat polymers increases the number of sites, where the negatively charged surfactants can be attached and, as a consequence, the polymer molecules become hydrophobized and form bigger and more compact aggregates. The presence of MAc in the BS solution decreases the size of aggregates for M100 and M295 and does not change the size of aggregates for the other polymer–surfactant mixtures studied.

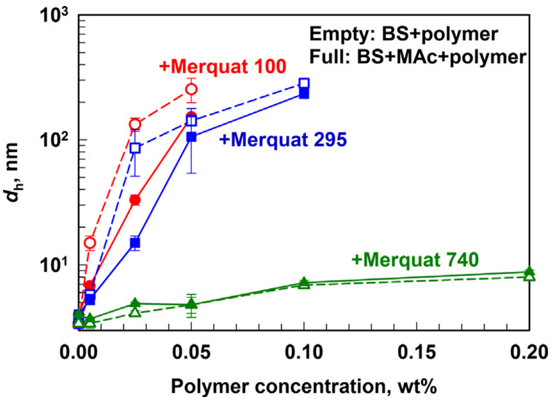

Fig. 1. Mean volume diameter of the aggregates, as a function of polymer concentration in BS + polymer (empty symbols) and BS + MAc + polymer (full symbols). Concentration of BS is 0.5 wt% and of MAc is 0.025 wt%.

The formation of smaller aggregates in mixed solutions with Lupasol polymers is due to the higher pH of these solutions, as compared to Merquat-containing solutions. Decreasing the pH of BS ± MAc + Lupasol G10 and BS ± MAc + Lupasol PS down to 6.5 led to heavy precipitates, due to the very high charge density of Lupasol molecules at this lower pH.

All discussed results so far were obtained at fixed polymer concentration of 0.1 wt% in the mixed solutions (except for M100 where the size of aggregates was measured at 0.05 wt% polymer, because the 0.1 wt% polymer solution was very turbid). The effect of polymer concentration on the aggregation in the mixed polymer–surfactant solutions was studied for M100, M295 and M740, see Fig. 1. The increase of polymer concentration increased significantly the aggregation in the mixtures with highly charged polymers (M100 and M295) and affected only slightly the aggregation in mixtures with M740 polymer which has the lowest charge density of 2.6 meq/g. A step-wise increase in aggregate size is observed for M100 and M295 at C_P = 0.025 wt%, where the concentration of positive charges is around 1.5 mM. For comparison, the concentration of negatively charged SLES molecules in the solution is ≈9.8 mM. Along with the total concentration of positive charges in the solution, significant impact on the aggregation has the distribution of these aggregates along the polymer chain—the aggregates in M740-containing mixtures are much smaller, as compared to aggregates in M100-containing solutions, at the same total charge concentration.

The presence of MAc in the polymer–surfactant solution decreases the size of the aggregates in solutions of highly charged polymers and does not affect the size for M740 containing solutions.

Viscosities of studied solutions. The viscosity of the studied solutions was measured by capillary viscometer. The experimental results are presented in Table S3. One sees that the viscosities of all studied polymer solutions are below 4 mPa.s. The highest viscosity is measured with M3330 (≈4.0 mPa.s), which has the highest molecular mass from the studied polymers from Merquat series (15×10^5 a.u.). The viscosities of the other polymer solutions from Merquat series varied between 1.2 and 2.1 mPa.s, depending on the molecular mass and charge density. The lowest viscosity is measured for M740, which has the lowest charge density and molecular mass. The viscosities of Lupasol solutions varied between 1.0 and 1.4 mPa.s. The highest viscosity is measured for Lupasol SK, which has the highest molecular mass of 20×10^5 Da. Therefore, the polymers from Merquat series increase to larger extent the solution viscosity, compared to Lupasol polymers, which is probably due to

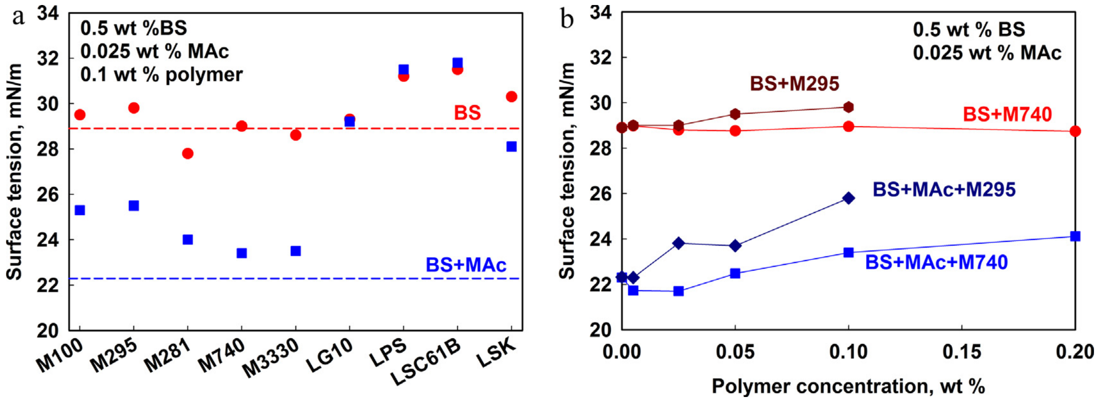

Fig. 2. Surface tension as a function of (A) used polymer in BS + polymer (red circles) and BS + MAc + polymer (blue squares) solutions and (B) polymer concentration for BS + Merquat 295 (dark red hexagons); BS + Merquat 740 (red circles); BS + MAc + Merquat 295 (dark blue diamonds) and BS + MAc + Merquat 740 (blue squares), as measured by Wilhelmy plate method after 900 s. The dashed red and blue lines in (A) represent the values for σ of 0.5 wt% BS and 0.5 wt% BS + 0.025 wt% MAc solutions, respectively. (For interpretation of the references to colour in this figure legend, the reader is referred to the web version of this article.)

the higher pH for Lupasol solutions and the related lower charge density of Lupasol polymers.

The viscosity of BS + polymer and BS + MAc + polymer solutions are slightly higher than the viscosity of the respective surfactant solutions (1 mPa.s) and noticeably lower than the viscosity of the polymer solutions, see the data in Table S3. For example, the viscosity of M295 decreases from 2 mPa.s to ≈1.1 mPa.s for BS + M295 and BS + MAc + M295 solutions. Similar trend is observed with the other polymers studied. The most probable explanation for the reduced viscosity of the polymer solutions in presence of SLES and CAPB is the attraction between the cationic polymers and the ionic surfactant molecules. Note that SLES is anionic surfactant which interacts with the cationic polymers and change their conformation and net charge density, thus shrinking the polymer molecules and decreasing solution viscosity. There is no significant difference in the viscosities of BS + polymer and BS + MAc + polymer solutions, which means that MAc of such low concentrations does not affect significantly the interaction between the polymer molecules.

3.2. *Surface properties*

3.2.1. *Equilibrium surface tension*

Fig. 2A presents the surface tension, as a function of the type of used polymer in the BS±MAc solutions. Surface tension of BS solution is slightly affected by the presence of M295 and M281, and noticeably affected when LPS, LSC61B or LSK is added to the solution. The effect of M295 and M281 is probably related to some interactions between the zwitterionic molecules of CAPB and the negatively charged acrylic acid in Merquat polymers. The noticeable effect of Lupasol polymers on surface tension of BS is due to the higher pH. To check this explanation we measured the surface tension of BS solution at pH 10. The measured surface tension is 31.4 mN/m, which is very close to the surface tension determined for BS + LPS and BS + LSC61B solutions (≈31.5 mN/m). The slightly lower surface tension measured for BS + LSK solution is related to the lower pH, measured with this solution (8.5). Therefore, we can conclude that Merquat polymers affect slightly the surface properties of BS solution, whereas the Lupasol polymers increase the surface tension of BS, due to the increased pH of the respective solutions.

The effect of polymers on the surface properties of BS + MAc solutions is much more pronounced. All studied polymers increase the surface tension of BS + MAc solution in different extends. The effect is the smallest for M3330, M740 and 281, which have charge density between 2.6 and 5.0 meq/g; intermediate for M100 and M295 and the largest for polymers from Lupasol series. Lupasols are able to increase the surface tension of BS + MAc up to the surface tension of BS solution. The only exception is LSK for which BS + MAc + LSK has somewhat lower surface tension than BS + LSK.

The intermediate effect of polymers from Merquat series (especially Merquat 100 and Merquat 295) can be explained by the attachment of some of MAc molecules to the polymer molecules in the bulk solution, so that the surface activity of MAc (which determines the low surface tension of BS + MAc system) decreases significantly and the properties of the adsorption layer are governed by the adsorbed SLES and CAPB molecules. To check this explanation we measured the surface tension, as a function of polymer concentration, for M295 and M740, see Fig. 2B. Surface tension of BS + MAc increases almost linearly with increasing M295 concentration, whereas it passes through a shallow minimum and increases afterwards for M740 containing solutions. The increase of surface tension for Merquat containing solution shows that these polymers interact with MAc molecules and decrease their adsorption activity.

There are at least three possible explanations for the significant effect of Lupasol polymers on surface properties of BS+MAc solution: (1) Increased pH (due to the presence of Lupasols in the solution) ionizes MAc molecules and the latter cannot form condensed surface phase on the bubble surfaces. (2) Lupasols bind MAc on their polymer chains in the bulk solution and the system behaves as there is no MAc on the solution surface. (3) Lupasols adsorb on the solution surface, form mixed adsorption layer with MAc, but the adsorbed polymer molecules perturb the structure of the MAc adsorption layer so that no surface condensed phase is formed. To distinguish between these explanations we performed experiments with BS + MAc + LSK and BS + MAc + LSC, in which we decreased the pH down to 6.5 when MAc molecules are non-ionized. The measured surface tension of BS + MAc + LSK and BS + MAc + LSC at pH 6.5 was 27.4 and 28.6 mN/m, respectively. Therefore, the main effect of Lupasol is not related to the ionization of MAc molecules, because the surface tension of BS + MAc + Lupasol solutions remain much higher than that of BS + MAc solution even at low pH. To distinguish between the second and third explanation we increased the concentration of MAc in the mixed solution up to 0.05 wt%. At this concentration the surface tension decreased down to 22 mN/m, which is a typical value for surface tension of BS + MAc solution. This experimental result clearly shows that the higher surface tension of BS + MAc + Lupasol mixture is due to binding of MAc molecules on the polymer chain. An excess of MAc is needed to compensate for the bound MAc molecules and to restore the MAc surface activity.

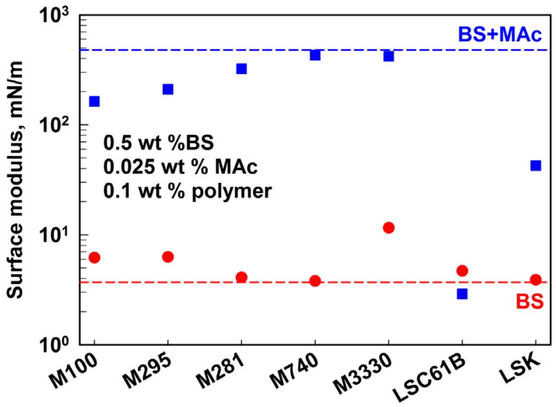

Fig. 3. Dilatational surface modulus, E for BS + polymer (red circles) and BS + MAc + polymer (blue squares) solution, as measured by ODM method. The dashed red and blue lines represent the values of E for 0.5 wt% BS and 0.5 wt% BS + 0.02 wt% MAc solutions, respectively. (For interpretation of the references to colour in this figure legend, the reader is referred to the web version of this article.)

3.2.2. Surface rheological properties

One of the most interesting properties of BS + MAc solutions is their high surface modulus [23–25]. To check how the polymers change the surface modulus of BS + MAc solutions, experiments with ODM method were performed by using the procedure described in Section 2.3. The obtained results are shown in Fig. 3. One sees that the surface modulus for BS + polymer solution is very close to the surface modulus for BS solution, which means that the studied polymers do not affect significantly the structure and composition of the adsorption layers of BS molecules. The only exception is M3330, which increases the surface modulus of BS solution from 3.7 to 11 mN/m, which is probably due to the adsorption of polymer–surfactant complexes on the solution surface.

On the other hand, all studied polymers have some effect on the surface properties of BS + MAc solution. The effect is the smallest for M3330 and M740. These two polymers decrease only slightly the surface modulus and increase slightly the surface tension. Therefore, they do not change significantly the structure and composition of the adsorption layer.

Noticeable effect on the surface modulus for BS + MAc is determined for the most charged polymers from Merquat series—M100 and M295. These two polymers decrease the surface modulus from 488 mN/m down to 160 mN/m. Nevertheless the surface moduli remain higher than 100 mN/m, which was found to be the threshold value for changing the rheological properties of foams in our previous study [25].

On the other hand, the addition of Lupasol SC and Lupasol SK to BS + MAc solutions decreases the surface moduli below 100 mN/m. The surface moduli of BS + MAc + LSC and BS + MAc + LSK solutions remain lower than 100 mN/m, even after decreasing the pH of the solution from natural to 6.5 (see Table S4), which shows that MAc is attached to Lupasol polymers in the solution and cannot form a condense adsorption layer on the solution surface. Therefore, along with the increased pH of the solutions, Lupasol SC61B and Lupasol SK bind MAc molecules and decrease their surface activity. As a consequence, the mixed adsorption layers formed at both studied pHs have low surface modulus.

The obtained results about the effect of Merquat 740 concentration on the surface modulus of BS and BS+MAc solutions are shown in Fig. 4. One sees that both surface loss modulus and surface storage modulus pass through a sharp maximum at M740 concentration around 0.025 wt%. Therefore, the effect of Merquat 740 on the surface rheological properties of BS + MAc solution depends strongly on polymer concentration and the largest effect is determined at 1:1 wt:wt ratio with respect to MAc molecules.

From these series of experiments we can conclude that: (1) Lupasol SC and Lupasol SK decrease the surface modulus of BS+MAc at both studied pH values (6 and 10) which is explained by binding of MAc molecules to the polymer chain, thus preventing the formation of condensed adsorption layer with high surface modulus. (2) Merquat molecules with high charge density (e.g. M100 and M295) decrease the surface modulus of BS + MAc from 480 to 160 mN/m, probably again interacting with MAc molecules in the solution. (3) Merquat with low charge density (M740) increases the surface modulus of BS+MAc, when added at 1:1 wt:wt ratio with MAc.

3.3. Foam film properties

3.3.1. Effect of Lupasols on the thinning of BS + MAc stabilized films

To check further the explanation that the Lupasol molecules bind MAc molecules in the bulk and reduce their surface activity, we observed the behaviour of foam films formed from BS + MAc + LSC and BS + MAc + LSK solutions. Illustrative consecutive images from the thinning of these foam films are shown in Fig. S1 in Supporting information. From the presented images, one sees that the films formed in the presence of polymers behave very differently from the films formed from BS solution alone. We observed much slower film thinning in the presence of polymers until the final equilibrium thickness of the films is reached (more than 300 s for BS + MAc + Lupasol SC; around 600 s BS + MAc + Lupasol SK, compared to 80 s for BS). Also, the foam films were thicker in the presence of polymers which shows that polymer molecules are adsorbed on the film surfaces.

In conclusion, formed molecular complexes of LSC + MAc and LSK + MAc are surface active and they are able to adsorb on the film surfaces, however, without preserving the high surface modulus, measured with BS + MAc systems in the absence of polymers.

3.3.2. Effect of M295 and M740 on the thinning of BS and BS + MAc stabilized films

The effect of polymers was studied in the concentration range between 0.005 wt% and 0.1 wt%. The main results from these experiments can be summarized as follows:

(1) The effect of Merquat 295 with respect to film thinning of BS stabilized films depends significantly on the polymer concentration and surface age. When $C_P \leq 0.025$ wt%, the films formed from BS + M295 thin down in a similar way, as those formed from BS solution only [23]. After film formation, the dimple disappears within several seconds and a foam film with uniform thickness of ≈100 nm is formed. Within the next 30 s, this film gradually thins down to ≈80 nm, when black spots are formed in the film area. These spots grow in size and for ≈10 s the film reaches its final equilibrium thickness of ≈40 nm. For these low polymer concentrations we did not observe any effect of the number of formed films on the film behavior. However, when $C_P \geq 0.05$ wt%, the film thinning behaviour depends significantly on the number of foam films formed. The first formed films behave similarly to those formed at low C_P. However, for every subsequent film we observed that the time for expanding of the black spots increases and the film thickness becomes more inhomogeneous, which indicates that more polymer molecules are attached to the film surfaces. At the highest polymer concentration studied, $C_P = 0.1$ wt%, we observed that the 4th formed film had inhomogeneous equilibrium thickness with formation of two-dimensional cellular structure—see the illustrative images in Fig. 5. Therefore, Merquat 295 adsorbs on the bubble surfaces for BS solution and is able to bridge the bubble surfaces in the sheared foams.

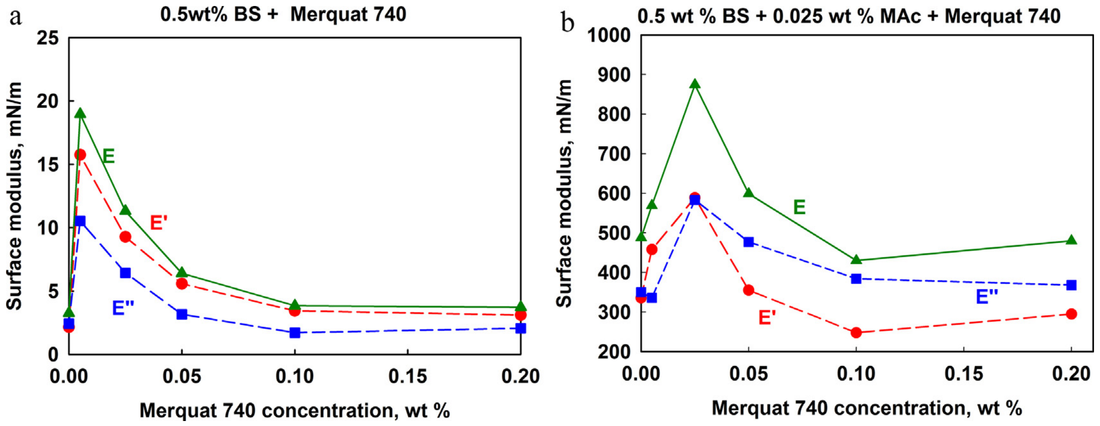

Fig. 4. Surface storage modulus, E' (red circles), surface loss modulus, E'' (blue squares), and total surface modulus, E (green triangles), as functions of Merquat 740 concentration in solution of (A) 0.5 wt% BS and (B) 0.5 wt% BS + 0.025 wt% MAc. These measurements are performed at 5 s period of oscillation. (For interpretation of the references to colour in this figure legend, the reader is referred to the web version of this article.)

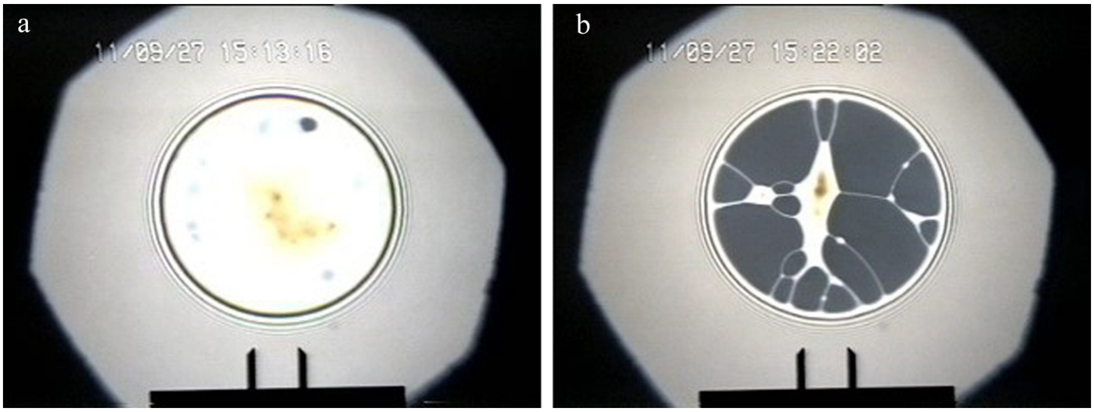

Fig. 5. Consecutive images for the 4th foam film, formed from 0.5 wt% BS + 0.1 wt% Merquat 295 solution (A) several seconds after film formation and (B) at equilibrium where two-dimensional cellular structure was formed inside the film. The distance between the two vertical bars is 50 μm.

(2) There is no significant effect of M295 on thinning behaviour of BS + MAc solutions, see illustrative pictures in Fig. S2. However, the final film thickness in presence of polymer is smaller as compared to film thickness of film formed from solution without polymer (30 vs 40 nm). The film thickness decrease is due to the fact that the polymer is polyelectrolyte and it increases the ionic strength of the solution and decreases the electrostatic repulsion between the film surfaces.

From this series we can conclude that Merquat 295 does not affect significantly the behavior of the BS + MAc foam films (except for the small reduction of the equilibrium film thickness). On the other hand, at $C_P \geq 0.05$ wt%, the presence of polymer in the BS solutions changes significantly the foam film behaviour.

(3) The effect of M740 on the behavior of BS films was also studied. Illustrative images from the stages of film thinning are shown in Fig. 6 and Fig. S3. One sees that, at the lowest Merquat concentration of 0.005 wt%, the system behaves like BS—see Fig. S3. At higher polymer concentrations, the equilibrium film thickness is larger which means that some trapped polymer between the film surfaces leads to steric stabilization of the film. At the highest polymer concentration, the film again thins down like there is no polymer in the system. Therefore, the film thickness of BS+M740 films passes through a maximum at $C_P \approx 0.025 \div 0.05$ wt.

(4) Experiments with BS + MAc + M740 solutions were also performed. Illustrative images from these experiments are shown in float element Fig. 6 or Fig. S4. One sees that at $C_P \leq 0.005$ wt%, the foam film behaves as that formed from BS + MAc, the only difference being the slightly lower equilibrium film thickness. However, when the concentration of M740 increases to 0.025 wt%, we observed the formation of foam films with non-uniform film thickness—part of the film area thickness close to the equilibrium one for BS + MAc, while other parts have thickness of ≈100 nm, see the white spots in the image shown in the fourth column and fourth row of Fig. S4. The further increase of M740 concentration leads to formation of films with structural patterns. At the highest studied M740 concentration, we observed worm-like pattern inside the film area.

3.4. Mean bubble size

A sample from the sheared foam at the end of each rheological experiment was taken and bubble size distribution was determined. The obtained experimental results for mean volume-surface radius, R_{32}, are shown in Fig. 7. All Lupasol polymers increase R_{32} from 150 μm to 300 μm for BS + MAc solutions. The later value is typical for bubbles formed from BS solutions at high pH. Therefore, Lupasols not only increase the surface tension of BS + MAc, decrease the surface modulus of BS + MAc, but also affect significantly the mean bubble size in sheared foams. Note that BS + MAc + LSK solution have surface modulus 46 mN/m which appears to insufficient

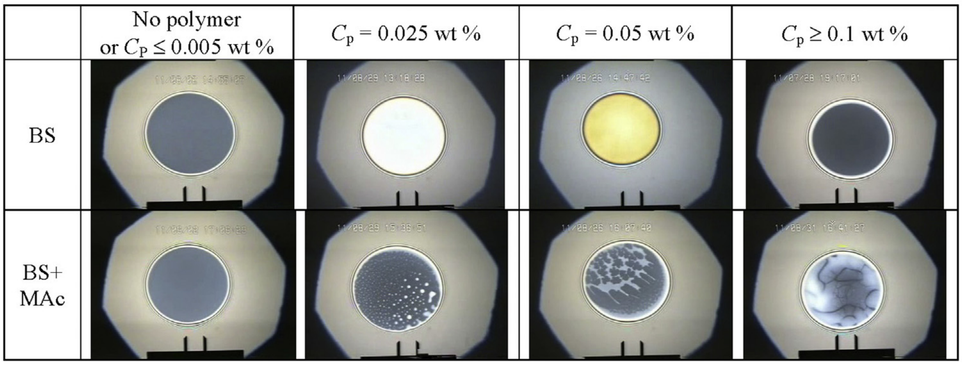

Fig. 6. Film with equilibrium thickness in closed cell formed from 0.5 wt% BS + Merquat 740 (second row) or 0.5 wt% BS + 0.025 wt% MAc + Merquat 740 (third row) at different polymer concentrations as indicated in first row. The distance between the two vertical bars is 50 μm.

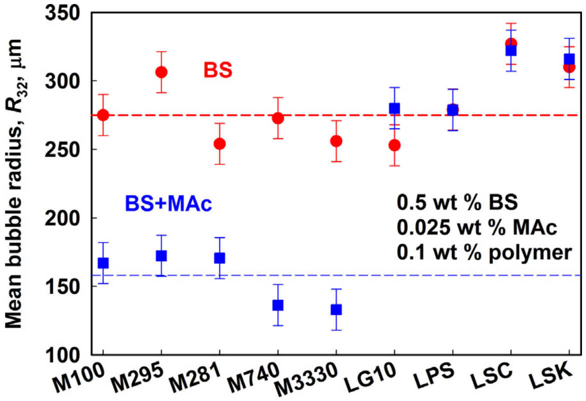

Fig. 7. Mean bubble size, R_{32}, in sheared foams, as a function of the polymer type: 0.5 wt% BS + 0.1 wt% polymer (red circles) and 0.5 wt% BS + 0.025 wt% MAc + 0.1 wt% polymer (blue squares). (For interpretation of the references to colour in this figure legend, the reader is referred to the web version of this article.)

to ensure small bubbles in the formed foam, in agreement with our previous results [26], where we showed that the threshold surface modulus for obtaining small bubbles in sheared foams is 100 mN/m.

As shown in Fig. 3, the surface modulus of BS + MAc + Merquat solutions depends on the surface charge of Merquat molecules. M100 decreases in greater extent the surface modulus of BS + MAc, whereas M740 and M3330 do not affect the surface modulus of BS+MAc. One sees that there is some small effect of M740 and M3330 on the mean bubble size for BS+MAc stabilized foams. The effect of M740 concentration on the mean bubble size is relatively small (see Fig. S5 in Supporting information). Therefore, the solutions which have surface modulus above 160 mN/m produce foams with mean bubble size of ≈150 μm under the conditions studied, whereas solutions with surface modulus lower than 100 mN/m produce foams with bubble size of ≈270 μm. The increase of surface modulus from 160 mN/m to 900 mN/m affects only slightly the mean bubble size in the foams formed.

3.5. *Foam rheology*

3.5.1. *Rheological properties of sheared foam*

The results from the rheological experiments with foams formed in BS ± MAc + polymer solutions were scaled, as described in Section 2.7 and fitted by Hershel–Bulkley equation for determination of the dimensionless yield stress, $\tilde{\tau}_0$ and flow index, n. The experimental results for all studied polymers are described well by the Hershel–Bulkley equation. In this Section, we present results for the effect of the studied polymers on the dimensionless yield stress (subsection A) and on the viscous friction inside foam (subsection B).

(A) Dimensionless yield stress

In our previous study [27] we showed that the dimensionless yield stress is strongly enhanced when Jaguar polymer is present in the foaming solution, whereas the presence of Merquat 100 does not affect the foam yield stress. The typical values for dimensionless yield stress for foams and emulsions with volume fraction $\Phi \approx 0.9$, are $\tilde{\tau}_0 = 0.033$ according to Princen [30] and $\tilde{\tau}_0 = 0.04$ to Mason [38].

The experimental results for the dimensionless yield stress for foams with air volume fraction of 90%, formed from various polymer + surfactant solutions, are shown in Fig. 8. Polymers from the Lupasol series increase slightly the dimensionless yield stress of BS ± MAc foams but the effect is relatively small—they increase $\tilde{\tau}_0$ from 0.04 to 0.05. The effect of the different Merquats on the dimensionless yield stress for BS and BS + MAc-stabilized foams, at $C_p = 0.1$ wt%, depends on the polymer type. Addition of M100, M281 or M3330 does not affect significantly the dimensionless yield stress of the foams—this stress remains in the range between 0.033 and 0.04 [30,38]. In contrast, significant increase of the dimensionless yield stress, up to 0.07, was observed when M740 was added to either of BS and BS + MAc solutions, and when M295 was added to BS solution, see Fig. 8.

The effect of polymer concentration on dimensionless yield stress was also studied and the results are shown in Fig. 8B. Merquat 295 does not affect the dimensionless yield stress for BS+MAc foams for all polymer concentrations studied, up to 0.1 wt%. At low $C_P \leq 0.025$ wt%, M295 does not affect the yield stress for BS foams as well. However, when this polymer is present in concentrations of 0.05–0.1 wt% in BS solution, it increases $\tilde{\tau}_0$ from 0.04 to 0.063 and 0.069, respectively. Therefore, Merquat 295 bridges the bubble surfaces in these systems when the adsorption layer contains SLES and CAPB, whereas it does not interact strongly with the adsorption layer containing predominantly MAc molecules. The difference in yield stress is due to the specific surface interactions between M295 and SLES or CAPB molecules, which is clearly seen from the experiments with foam films, where we observed that M295 changes the thinning behaviour of films formed from BS solution, see Fig. 5, whereas it does not affect the thinning of the films formed from BS + MAc solutions, see Fig. S2 in supporting information.

The effect of M740 on $\tilde{\tau}_0$ is also seen in Fig. 8B. This polymer affects significantly the dimensionless yield stress of BS and BS + MAc solutions. For BS + MAc + M740 stabilized foams, the dimensionless yield stress increases almost linearly with the increase of C_P in the range between 0.005–0.2 wt% and reaches the value of 0.085. This high dimensionless foam yield stress is

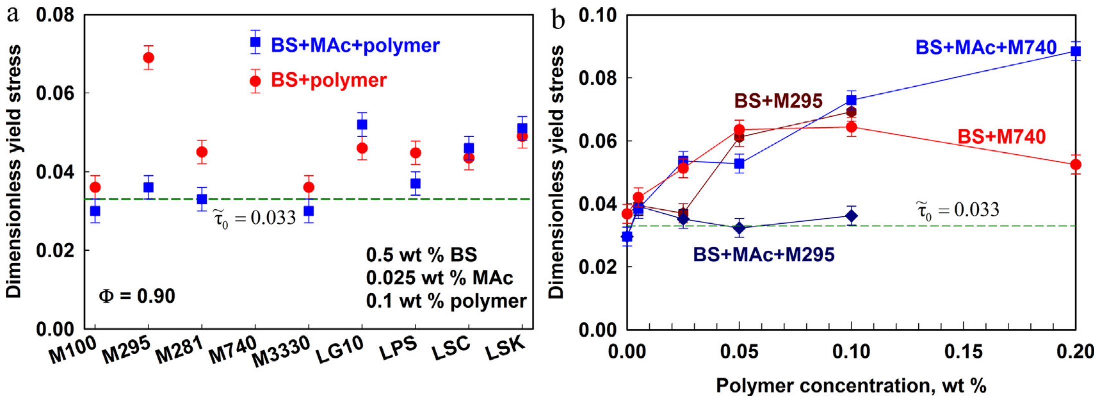

Fig. 8. Dimensionless yield stress as a function of (A) type of polymer and (B) concentration of polymer in foaming solution used for foam generation with air volume fraction of 90%.

close to the value measured with Jaguar C13s-containing solutions [27]. When the concentration of M740 increases in the BS solutions, initially $\tilde{\tau}_0$ increases from 0.04 to 0.065 with the increasing of C_P to 0.05 wt%, remains constant in the range 0.05–0.1 wt%, and decreases with the further increase of C_P up to 0.2 wt%. Therefore, the effect of M740 is more pronounced for BS + MAc solutions which could be explained with the stronger interactions between M740 and MAc molecules, compared to the interactions between M740 and SLES + CAPB molecules. These results are in a very good agreement with the foam film observations, where we found that the thickness of the film passes through a maximum with increasing the polymer concentration for BS + M740, see Fig. 6, whereas for BS + MAc + M740 we observe a gradual increase in the fraction of film area occupied by polymer molecules, see the white spots in Fig. 6B.

From this series of experiments we can conclude that the presence of polymers in the adsorption layer, which in their own turn affect the interactions between the film surfaces, has significant impact on the dimensionless yield stress of the foams formed.

- Dimensionless viscous stress

The results for the dimensionless viscous stress, as a function of the capillary number, for foams prepared from Lupasol-containing solutions, are shown in Fig. S6. One sees that the data for Lupasols fall close to the master line for BS solution (system with low surface modulus) with power law index $n \approx 0.44$. Therefore, the Lupasol polymers are able to suppress the effect of myristic acid on the surface and foam properties of the system by binding MAc molecules in the bulk solution and preventing the formation of surface condensed phase.

The effect of pH for BS + MAc + Lupasol mixtures on foam viscous friction was also studied. The decrease of pH to 6.5 for BS + MAc + Lupasol mixtures does not restore the surface modulus of BS+MAc solution, see Fig. S7, which proves that the suppression of the cosurfactant effect of MAc is not due to the higher pH of Lupasol solutions. To check whether the increase of MAc concentration in the solution could restore its effect on the foam rheological properties, we performed experiments at twice higher MAc concentration, 0.05 wt%, at which the surface tension was 22 mN/m. The obtained results are shown in Fig. S8 and they clearly show that two times increase of MAc is sufficient to restore completely its effect on the foam properties in the presence of 0.1 wt% Lupasol.

Experimental results for the flow index, n, as determined from the best fits to the rheological curves by Hurshel–Bulkley equation, are shown in Fig. 9A. Merquat polymers slightly affect the rheological response of BS foams, whereas significant effect of M740 is determined for BS + MAc foam. Merquat 740 is able to increase the flow index from 0.25 (typical value for foams with high surface modulus) up to 0.32, which is an intermediate flow index between those for high and low surface moduli, respectively. The effect of polymer concentration is also studied, see Fig. 9B. Merquat 295 does not affect the viscous friction for both BS and BS + MAc stabilized foams, whereas this polymer has significant impact on yield stress of BS foams. On the other hand Merquat 740 does not affect the properties of BS foams, but increases significantly the flow index for BS + MAc foams. Significant increase in the flow index for BS + MAc foams with increasing of M740 concentration in the solution is most probably related to adsorption of polymer–surfactant complexes on the bubble surfaces as visible from the images presented in Fig. 6. The adsorbed polymers increase significantly the yield stress of the foams, but decrease the viscous friction, which is also clearly seen from data presented in Fig. S10. Probably, at low shear rates, the adsorbed polymer molecules bridge the bubble surfaces and enhance the foam yield stress. At higher shear rate, however, the presence of polymers in the adsorption layer disrupts the condensed adsorption layer and the flow index increases.

From all these experiments we can conclude that (1) Lupasol polymers increase pH up to 10, MAc molecules become ionized and cannot form condensed adsorption layer on the bubble surface. (2) Even after decreasing pH down to 6.5, the cosurfactant effect of MAc remains negligible for BS + MAc + Lupasol solutions, which is attributed to binding of MAc molecules to the polymer molecules in the solution. At this pH the effect of MAc can be restored after increasing twice its concentration in the solution. (3) The only polymer from Merquat series which affects significantly the foam viscous friction is M740 which has the lowest charge density. Increasing its concentration in BS + MAc solution leads to higher yield stress, which at $C_P \geq 0.1$ wt% is accompanied with an apparent decrease of the viscous friction.

3.5.2. *Friction between foam and solid wall*

Results for the dimensionless wall stress, obtained with BS and BS + MAc systems containing different polymers, are compared in Fig. 10. One sees that the experimental data for foams, stabilized with BS + polymer, merge around a master line with a power-law index $m \approx 2/3$, which indicates that the bubbles surface in all these mixtures is tangentially mobile, Fig. 10A. The data for the dimensionless wall stress in the experiments with BS + MAc + polymer solutions agree with the results about inside-foam friction: For BS + Merquat systems, the dimensionless wall stress merges around a master line with a power-law $m \approx 1/2$, typical for the systems containing MAc, whereas the data for Lupasols fall on the master line for BS with power-law index $n \approx 2/3$. The addition of 0.1 wt% M740 leads to the appearance of a minimum in the curve τ_W vs. Ca^*. The appearance of this minimum can be explained in

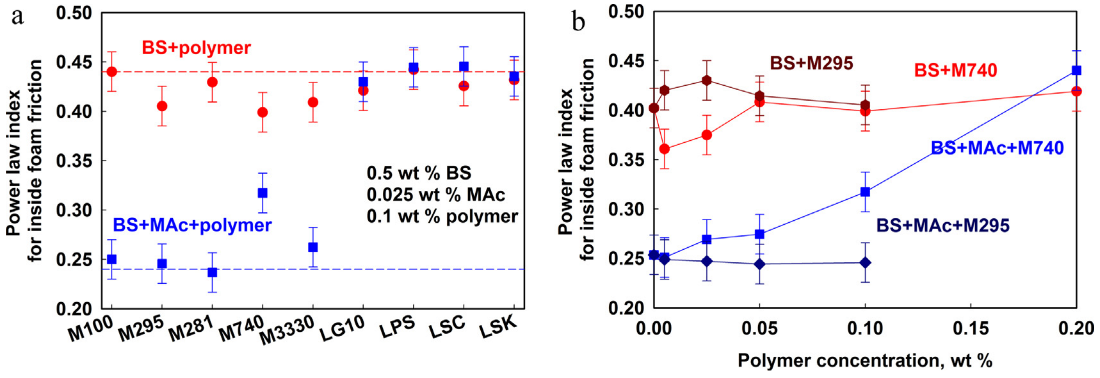

Fig. 9. Power law index for inside foam friction, *n*, as a function of (A) type of polymer and (B) concentration of polymer in foaming solution used for foam generation with air volume fraction of 90%.

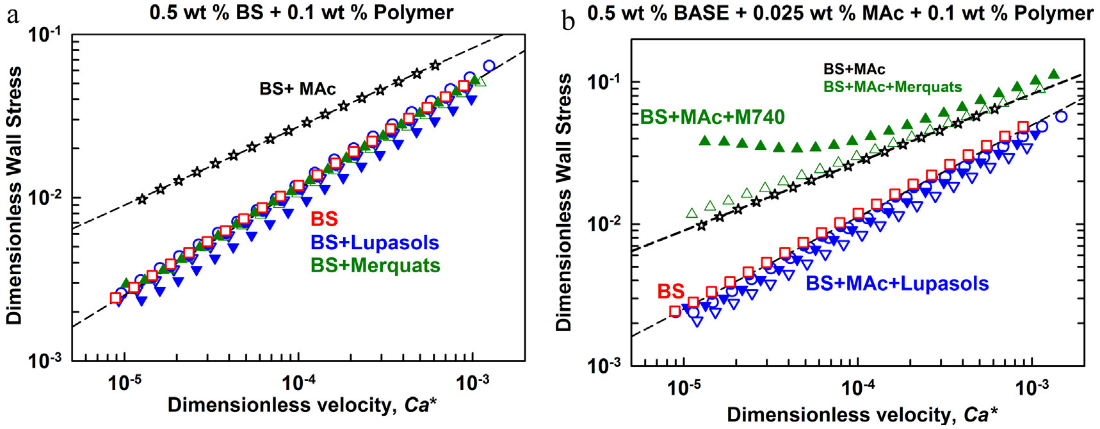

Fig. 10. Dimensionless wall stress, as a function of dimensionless velocity, for foam-wall friction in (A) 0.5 wt% BS + 0.1 wt% Polymer and (B) 0.5 wt% BS + 0.025 wt% MAc + 0.1 wt% Polymer. The different types of polymers are denoted as follows: Lupasols (blue symbols), Merquats (green symbols). Air volume fraction for all studied foams is 0.9. (For interpretation of the references to colour in this figure legend, the reader is referred to the web version of this article.)

the following way [27]: The molecules of the cationic polymer form strong bridges between the bubbles and the solid wall (see Fig. 8 in Ref. [27]). In this way, the bubbles are attached to the surface of the plate. As the plate starts moving, an elastic component in the wall stress appears at low velocity, due to the stretching of the polymer chains. As the sliding progresses, a certain “wall yield stress” is exceeded, and the bubbles are detached from the wall. The measured stress is now due to the foam/wall viscous friction, and the plot merges with that of the polymer-free system.

The results for foam-wall friction with added Merquat 740 in BS + MAc foams strongly supports our hypothesis that, after destruction of the polymer bridges, they do not affect the flow curve any further. Note that, if there was any effect of this apparent yield stress on the flow curve at high shear rates, then the curve for the dimensionless wall stress for BS + MAc + M740 would lie above the other curves (which is not observed, see Fig. 10B). Another interesting point here is that the presence of M740 or M295 in BS solutions does not affect the foam-wall friction, despite the fact that these polymers increase significantly the foam yield stress in these systems, see Fig. 8 above. Further discussion on this point is presented in the next paragraph, after presenting the results about the effect of the concentration of these polymers on the foam-wall friction.

The results about the effect of M740 and M295 concentration on the foam-wall friction for BS and BS+MAc stabilized foams, are shown in Fig. 11. The presence of M740 or M295 at concentrations up to 0.2 wt% in the foaming solution does not affect the rheological properties of the BS stabilized foams. On the other hand, well pronounced plateau region is observed in the flow curves for BS + MAc + M740 systems at $C_P \geq 0.05$ wt%. Therefore, specific interactions exist between M740 and MAc. Note that we observed similar effect in our previous study [27] for the systems containing Jaguar C-13s, but well pronounced yield stress in wall-foam friction was determined for all studied systems containing Jaguars (BS, BS + cosurfactants with LSM and BS + cosurfactant with HSM). Thus, we can expect that Jaguars interact with the main surfactants (SLES and/or CAPB) in the solution, whereas M740 interacts specifically with MAc.

4. Conclusions

The performed experiments with two series of cationic polymers and the surfactant systems SLES + CAPB ± MAc (BS ± MAc) allowed us to formulate the following conclusions:

(1) Polymers from Lupasol series increase pH of the solutions up to 10, due to polymer- induced hydrolysis of water. Lupasols suppress the cosurfactant effect of MAc on all surface and foaming properties, such as surface rheological properties, inside-foam friction, foam-wall friction, and mean bubble size. These polymers suppress the effect of MAc even after decreasing pH down to 6.5. However, two times increase of MAc concentration (from 0.025 to 0.05 wt%) at fixed polymer concentration of 0.1 wt% restores completely the MAc cosurfactant effect on the surface and foam properties at pH 6.5. These results show that Lupasol polymers are able to bind strongly MAc molecules in the bulk solution, thus reducing their surface activity. An excess of MAc molecules is needed to saturate the dissolved Lupasol

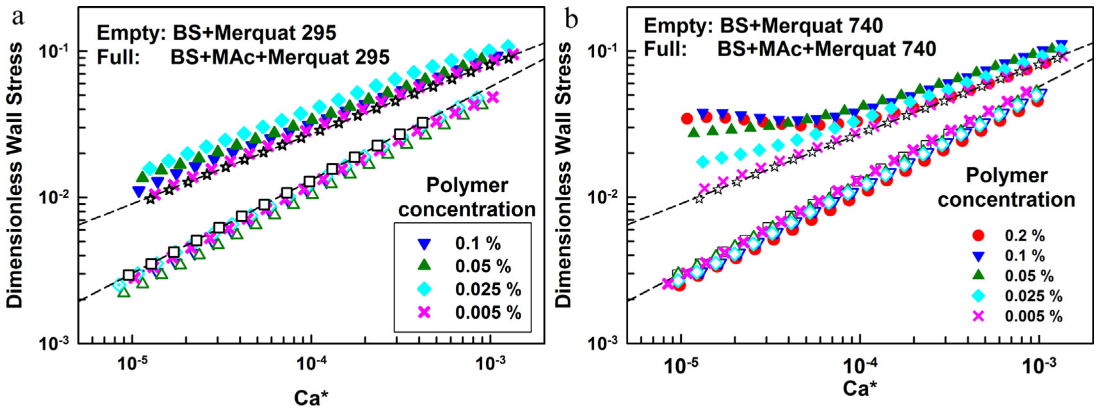

Fig. 11. Dimensionless wall stress, as a function of dimensionless velocity, for foam-wall friction in (A) 0.5 wt% BS + Merquat 295 (empty symbols) and 0.5 wt% BS + 0.025 wt% MAc + Merquat 295 (full symbols) and (B) 0.5 wt% BS + Merquat 740 (empty symbols) and 0.5 wt% BS + 0.025 wt% MAc + Merquat 740 (full symbols) with different polymer concentrations denoted as follows: 0.2 wt%(red symbols); 0.1 wt% (blue symbols); 0.05 wt% (green symbols); 0.025 wt% (cyan symbols); 0.005 wt% (pink symbols). (For interpretation of the references to colour in this figure legend, the reader is referred to the web version of this article.)

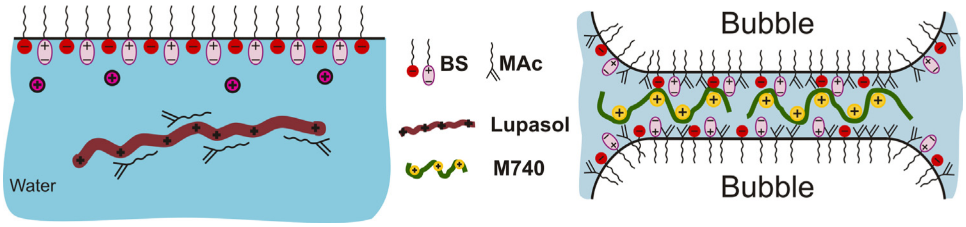

Fig. 12. Schematic representation of (A) Adsorption of MAc molecules on Lupasol polymer chain, which leads to fact that surface properties are governed by SLES and CAPB molecules; (B) Adsorption of Merquat 740 over surfactant adsorption layer, which bridges the film surfaces and increases the foam yield stress.

polymer chains and to restore the surface activity of MAc as a cosurfactant.

(2) Merquat 740 (copolymer with low charge density) has significant effect on the dimensionless foam yield stress, foam-wall friction, and thinning behaviour of foam films in BS + MAc system. These effects are related to strong interactions between MAc and polymer molecules in the adsorption layers, as evidenced by measured surface properties and by foam film observations. For BS foams, M740 has effect only on the dimensionless foam yield stress, when the polymer concentration is between 0.025 and 0.05 wt%—the polymer is able to bridge the foam film surfaces in this relatively narrow concentration range only.

(3) Merquat 295 (copolymer with higher charge density which contains a small fraction of acrylic acid units) increases significantly the dimensionless yield stress for BS foams, when it is present in a concentration of 0.05 wt% and above. However, it has no any effect on BS + MAc foams which shows that this polymer interacts with SLES and/or CAPB only.

(4) Merquat 100 (homopolymer with very high charge density) adsorbs on the bubble surfaces but forms a very thin (flat) adsorption layer which does not bridge the foam film surfaces. As a result, this polymer does not affect the main foam properties.

(5) The other studied polymers have no significant effect on any of the studied properties (surface rheological modulus, friction inside foam, foam-wall friction and mean bubble size).

Thus we conclude that a wide range of polymer–surfactant–cosurfactant interactions are possible which, in turn, affect the surface and foam properties. All observed effects of the cationic polymers on foam properties could be explained by considering two important phenomena (see Fig. 12):

First, one should consider the competition between the polymer adsorption on the surfactant adsorption layer and the surfactant binding to the polymer molecules in the bulk solution. In our systems, the strong polymer–cosurfactant interactions in the bulk solution led to the suppression of the cosurfactant effect of MAc in Lupasol-containing solutions, due to the MAc binding to dissolved Lupasol molecules (Fig. 12A).

Second, one should consider the thickness of the formed polymer–surfactant adsorption layers—if this thickness is comparable to the foam film thickness, the polymer is able to bridge the foam film surfaces and to increase the foam yield stress (similarly for the wetting films between bubbles and confining solid wall and the related foam-wall yield stress). Thicker adsorption layers are formed at lower polymer charge density and higher polymer mass. In contrast, thin polymer adsorption layers, formed at high charge density of the polymer molecules, do not bridge the bubble surfaces and the foam yield stress is not affected by the adsorbed polymer.

Acknowledgments

The authors are grateful to Mrs. Julieta Vulkova for the measurements of surface modulus and Mrs. Kristina Rusanova for the foam film thinning experiments (both from Sofia University). The study is supported by Unilever R&D Center in Trumbull, USA.

Appendix A. Supplementary data

Supplementary data associated with this article can be found, in the online version, at http://dx.doi.org/10.1016/j.colsurfa.2015.10.034.

References

[1] Application of Surfactants with Polymers and Proteins, in: E.D. Goddard, K.P. Ananthapadmanabhan (Eds.), CRC Press, Boca Raton, FL, 1993.

[2] E.D. Goddard, K.P. Ananthapadmanabhan (Eds.), Application of Polymer–surfactant Systems. Surfactant Science Series, vol. 77, Marcel Dekker, 1998, 2015.

[3] P. Hansson, Interaction between polyelectrolyte gels and surfactants of opposite charge, Curr. Opin. Colloid Interface Sci. 11 (2006) 351.

[4] D. Langevin, Complexation of oppositely charged polyelectrolytes and surfactants in aqueous solutions. A review, Adv. Colloid Interface Sci. 147–148 (2009) 170.

[5] A. Mezei, R. Meszaros, Novel method for the estimation of the binding isotherms of ionic surfactants on oppositely charged polyelectrolytes, Langmuir 22 (2006) 7148.

[6] C.D. Bain, P.M. Claesson, D. Langevin, R. Meszaros, T. Nylander, C. Stubenrauch, S. Titmuss, Complexes of surfactants with oppositely charged polymers at surfaces and in bulk, Adv. Colloid Interface Sci. 155 (2010) 32.

[7] X.L. Zhang, D.J.F. Taylor, R.K. Thomas, J. Penfold, Adsorption of polyelectrolyte/surfactant mixtures at the air–water interface: modified poly(ethyleneimine) and sodium dodecyl sulfate, Langmuir 27 (2011) 2601.

[8] D. Langevin, F. Monroy, Interfacial rheology of polyelectrolytes and polymer monolayers at the air–water interface, Curr. Opin. Colloid Interface Sci. 15 (2010) 283.

[9] D.J.F. Taylor, R.K. Thomas, J. Penfold, Polymer/surfactant interactions at the air/water interface, Adv. Colloid Interface Sci. 132 (2007) 69.

[10] J. Penfold, R.K. Thomas, D.J.F. Taylor, Polyelectrolyte/surfactant mixtures at the air-solution interface, Curr. Opin. Colloid Interface Sci. 11 (2006) 337.

[11] T. Nylander, Y. Samoshina, B. Lindman, Formation of polyelectrolyte–surfactant complexes on surfaces, Adv. Colloid Interface Sci. 123–126 (2006) 105.

[12] A. Rao, J. Kim, R. Thomas, Interfacial rheological studies of gelatin–sodium doedecyl sulfate complexes adsorbed at the air–water interface, Langmuir 21 (2005) 617.

[13] C. Monteux, M.-F. Liauro, D. Baigl, C.E. Williams, O. Anthony, V. Bergeron, Interfacial microgels formed by oppositely charged polyelectrolytes and surfactants. 1. Influence of polyelectrolyte molecular weight, Langmuir 20 (2004) 5358.

[14] C. Monteux, C.E. Williams, V. Bergeron, Interfacial microgels formed by oppositely charged polyelectrolytes and surfactants. 1. Influence of surfactant chain length and surfactant/polymer ratio, Langmuir 20 (2004) 5367.

[15] C. Monteux, G.G. Fuller, V. Bergeron, Shear and dilational surface rheology of oppositely charged polyelectrolyte/surfactant microgels adsorbed at the air–water interface. Influence on foam stability, J. Phys. Chem. B 108 (2004) 16473.

[16] B.A. Noskov, G. Loglio, R. Miller, Dilational surface visco-elasticity of polyelectrolyte/surfactant solutions: formation of heterogeneous adsorption layers, Adv. Colloid Interface Sci. 168 (2011) 179.

[17] A.M. Díez-Pascual, F. Monroy, F. Ortega, R.G. Rubio, R. Miller, B.A. Noskov, Adsorption of water-soluble polymers with surfactant character. Dilational viscoelasticity, Langmuir 23 (2007) 3802.

[18] C. Üzüm, N. Kristen, R. von Klitzing, Polyelectrolytes in thin liquid films, Curr. Opin. Colloid Interface Sci. 15 (2010) 303.

[19] R. von Klitzing, Effect of interface modification on forces in foam films and wetting films, Adv. Colloid Interface Sci. 114-115 (2005) 253.

[20] B. Jean, L.-T. Lee, B. Cabane, V. Bergeron, Foam films from thermosensitive PNIPAM and SDS solutions, Langmuir 25 (2009) 3966.

[21] R. Petkova, S. Tcholakova, N. Denkov, Foaming and foam stability for mixed polymer–surfactant solutions: effects of surfactant type and polymer charge, Langmuir 28 (2012) 4996.

[22] R. Petkova, S. Tcholakova, N. Denkov, Foaming and foam stability for mixed polymer–surfactant solutions: effects of pH and surfactant head group for cationic polyvinylamine and anionic surfactants, Colloids Surf. A 438 (2013) 174.

[23] K. Golemanov, N.D. Denkov, S. Tcholakova, M. Vethamuthu, A. Lips, Surfactant mixtures for control of bubble surface mobility in foam studies, Langmuir 24 (2008) 9956.

[24] Z. Mitrinova, S. Tcholakova, J. Popova, N. Denkov, B. Dasgupta, M. Vethamuthu, K.P. Ananthapadmanabhan, Efficient control of the rheological and surface properties of surfactant solutions containing C8–C18 fatty acids as cosurfactants, Langmuir 29 (2013) 8255.

[25] Z. Mitrinova, S. Tcholakova, K. Golemanov, N. Denkov, M. Vethamuthu, K.P. Ananthapadmanabhan, Surface and foam properties of SLES + CAPB + Fatty acid mixtures: effect of pH for C12–C16 acids, Colloids Surf. A 438 (2013) 186.

[26] S. Tcholakova, Z. Mitrinova, K. Golemanov, N. Denkov, M. Vethamuthu, K.P. Ananthapadmanabhan, Control of ostwald ripening by using surfactants with high surface modulus, Langmuir 27 (2011) 14807.

[27] N. Politova, S. Tcholakova, K. Golemanov, N.D. Denkov, M. Vethamuthu, K.P. Ananthapadmanabhan, Effect of cationic polymers on foam rheological properties, Langmuir 28 (2012) 1115–1126.

[28] P.R. Garrett, J.D. Hines, S.C. Joyce, P.T. Whittal, Report prepared for Unilever R&D, Port Sunlight (1993).

[29] S. Mukherjee, H. Wiedersich, Morphological and viscoelastic properties of dense foams generated from skin cleansing bars, Colloids Surf. A 95 (1995) 159.

[30] H.M. Princen, The structure, mechanics, and rheology of concentrated emulsions and fluid foams, in: J. Sjöblom (Ed.), Encyclopedia of Emulsion Technology, Marcel Dekker, New York, 2001, p. 243 (Chapter 11).

[31] D. Weaire, The rheology of foam, Curr. Opin. Colloid Interface Sci. 13 (2008) 171.

[32] A.M. Kraynik, Foam flows, Ann. Rev. Fluid Mech. 20 (1988) 325.

[33] H.M. Princen, Rheology of foams and highly concentrated emulsions: I. Elastic properties and yield stress of a cylindrical model system, J. Colloid Interface Sci. 91 (1983) 160.

[34] H.M. Princen, Rheology of foams and highly concentrated emulsions. II. Experimental study of the yield stress and wall effects for concentrated oil-in-water emulsions, J. Colloid Interface Sci. 105 (1985) 150.

[35] H.M. Princen, A.D. Kiss, Rheology of foams and highly concentrated emulsions: IV. An experimental study of the shear viscosity and yield stress of concentrated emulsions, J. Colloid Interface Sci. 128 (1989) 176.

[36] N.D. Denkov, V. Subramanian, D. Gurovich, A. Lips, Wall slip and viscous dissipation in sheared foams: effect of surface mobility, Colloids Surf. A 263 (2005) 129.

[37] A. Scheludko, Thin liquid films, Adv. Colloid Interface Sci. 1 (1967) 391.

[38] T.G. Mason, J. Bibette, D.A. Weitz, Yielding and flow of monodisperse emulsions, J. Colloid Interface Sci. 179 (1996) 439.